LETTERS
PUBLISHED ONLINE: 1 JULY 2012 | DOI: 10.1038/NPHYS2353
nature physics

Ultrafast entangling gates between nuclear spins using photoexcited triplet states

Vasileia Filidou[1†], Stephanie Simmons[1†], Steven D. Karlen[1,2], Feliciano Giustino[1], Harry L. Anderson[2] and John J. L. Morton[1,3*]

The representation of information within the spins of electrons and nuclei has been a powerful method in the ongoing development of quantum computers[1,2]. Although nuclear spins are advantageous as quantum bits (qubits) because of their long coherence lifetimes (exceeding seconds[3]), they exhibit very slow spin interactions and have weak thermal polarization. A coupled electron spin can be used to polarize the nuclear spin[4–6] and create fast single-qubit gates[7,8], however, the permanent presence of electron spins is a source of nuclear decoherence. Here we show how a transient electron spin, arising from the optically excited triplet state of C_{60}, can be used to hyperpolarize, manipulate and measure two nearby nuclear spins. Implementing a scheme that uses the spinor nature of the electron[9], we performed an entangling gate in hundreds of nanoseconds: five orders of magnitude faster than the liquid-state *J* coupling. This approach can be widely applied to systems comprising an electron spin coupled to multiple nuclear spins, such as nitrogen–vacancy centres in diamond[10], while the successful use of a transient electron spin motivates the design of new molecules able to exploit photoexcited triplet states.

Different quantum systems possess different advantages as qubits, stimulating the use of so-called hybrid approaches to quantum computing[11]. Examples include interfacing superconducting qubits with spin ensembles[12], optical photons with defects in solids[13], and electron spins with nuclear spins[3]. Spins controlled by nuclear magnetic resonance (NMR) have played an important role in the development of much experimental work in quantum information processing, showcasing high-fidelity control[14], complex demonstrations of quantum algorithms[15] and many-qubit decoupling strategies[16]. Nuclei in such systems are only weakly coupled: the indirect *J*-coupling interaction available in liquid-state NMR can be on the order of 100 Hz (ref. 15), although nuclear spin dipole couplings in the solid state can exceed 10 kHz.

This weak coupling places a lower limit on the duration of a quantum logic operation between two spins, and thus the computational speed of a nuclear spin-based quantum information processor. Furthermore, the weak magnetic moment of nuclear spins leads to a weak polarization in general (typically less than 0.01% for liquid state NMR), making the scaling-up of the initial demonstrations very challenging unless a method for nuclear spin cooling can be applied[17].

These limitations can be addressed by making use of a coupled electron spin. Highly polarized electron spin states can be transferred to the nuclear spin coherently using SWAP operations[3,6,18], or incoherently using a family of dynamic nuclear polarization methods[4,5]. Typical single-qubit gate times for electron spins are tens of nanoseconds and, given typical electron–nuclear couplings (in the range 1–100 MHz), it is possible to manipulate a nuclear spin on these timescales. For purely isotropic couplings, phase gates can be applied to nuclear spin qubits to perform dynamic decoupling[7,19], whilst using anisotropic coupling, more general gates have been applied to single nuclear spins[8,20,21], or, recently, two nuclear spins[22].

A disadvantage of using coupled electron spin is that the nuclear spin coherence time can be strongly limited by electron spin relaxation or flip-flop processes[3]. A better strategy invokes an electron spin only at certain key times, for example to hyperpolarize the nuclear spins or to perform fast logic gates, so that there is minimal long-term impact on nuclear decoherence[23].

To explore such possibilities, we synthesised the fullerene derivative dimethyl[9-hydro(C_{60}-I_h)[5,6]fulleren-1(9H)-yl)phosphonate (DMHFP; ref. 24), illustrated in Fig. 1a, containing two nuclear spins (^{31}P and ^{1}H) which are directly bonded to a C_{60} fullerene cage. The molecule has a diamagnetic singlet ground state which can be photoexcited to populate the first excited singlet state. This state undergoes intersystem crossing (ISC) to a hyperpolarized, long-lived triplet state which is paramagnetic ($S=1$) with electron spin density delocalized over the cage (Fig. 1b,c). This system provides all the ingredients to explore nuclear spin manipulations mediated by a transient electron spin using a combination of optical excitation, electron spin resonance (ESR) and NMR control.

We begin by characterizing the spin Hamiltonian, $\mathcal{H}$, of the DMHFP molecule:

$$\mathcal{H} = \mu_B \mathbf{S}\cdot g_e \cdot \mathbf{B} + \mathbf{S}\cdot D\cdot \mathbf{S} + \sum_{i=^{31}\mathrm{P},^{1}\mathrm{H}} \mathbf{S}\cdot A_i \cdot \mathbf{I}_i + J I_{1,z} I_{2,z} + \gamma_{i,n} \mathbf{I}_i \cdot \mathbf{B} \quad (1)$$

where **S** and **I** are respectively the electron and nuclear spin operators, **B** is the applied magnetic field, $\gamma_{i,n}$ the nuclear gyromagnetic ratio, g_e the electron g-factor tensor, μ_B the Bohr magneton, D the zero-field splitting (ZFS) tensor for the $S=1$ triplet state, A_i the hyperfine coupling tensor between the triplet and the nuclear spins i, and J is the coupling between the nuclear spins. I_i, z is the projection of **I** along z. All terms involving **S** vanish in the electronic ground state.

By performing pulsed ESR immediately following a 532 nm laser pulse we examine the properties of the triplet state. Figure 1d shows the intensity of an electron spin echo as a function of the applied magnetic field in the X-band (9.7 GHz microwave frequency). By comparing the spectrum to simulations[25], we obtain the g_e-tensor

[1]Department of Materials, University of Oxford, Parks Road, Oxford OX1 3PH, UK, [2]Department of Chemistry, University of Oxford, Oxford OX1 3TA, UK, [3]CAESR, The Clarendon Laboratory, Department of Physics, University of Oxford, Oxford OX1 3PU, UK. †These authors contributed equally to this work. *e-mail: john.morton@materials.ox.ac.uk.

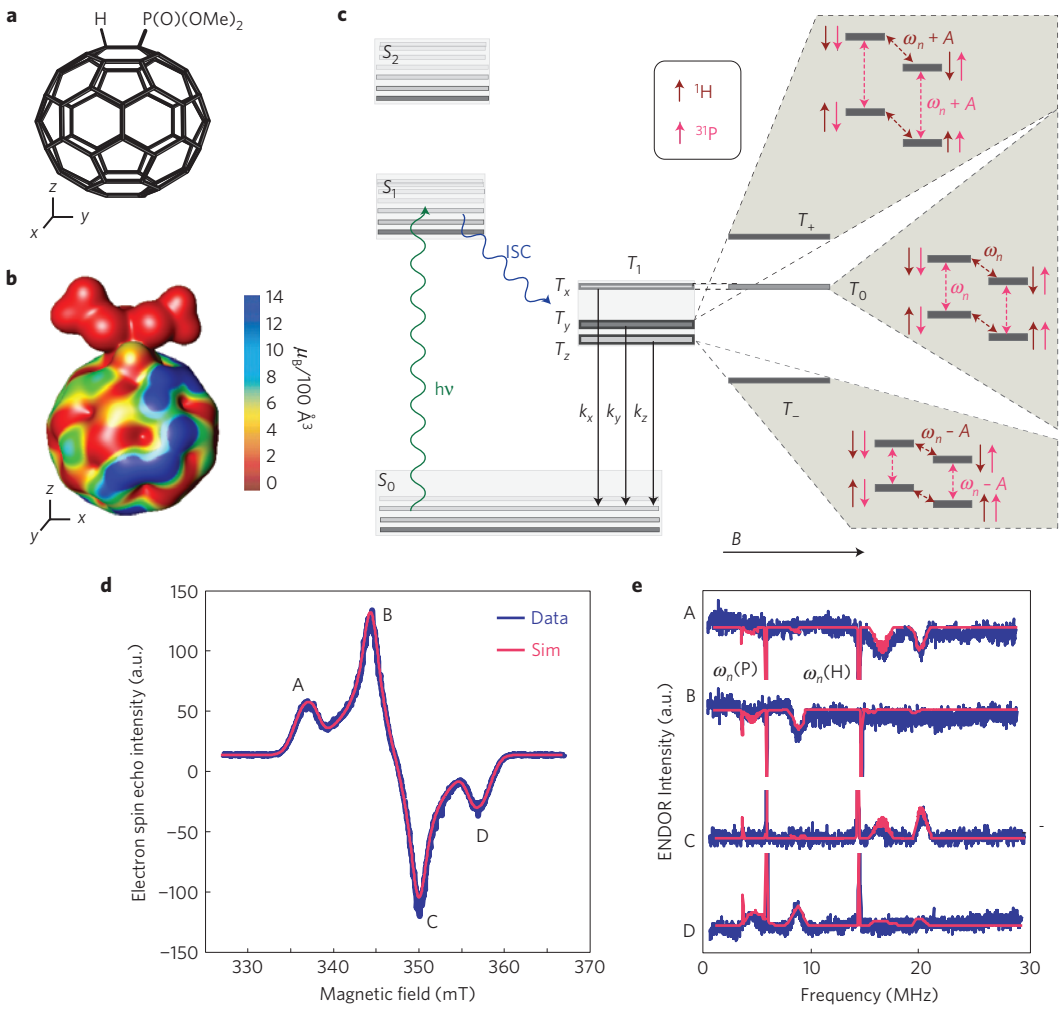

Figure 1 | The DMHFP molecule has an excited triplet state which couples to two nuclear spins: ^{1}H and ^{31}P. a, Illustration of the DMHFP molecule. **b**, Spin density distribution in the excited triplet state T_1, where blue areas correspond to atoms with high electron spin density. **c**, The system has a diamagnetic singlet ground state S_0 which can be excited through ISC to a triplet state, T_1. The application of a magnetic field mixes the triplet sublevels in an orientation-dependent manner. The triplet further couples to the two nuclear spins directly bonded to the cage, causing further splittings due to nuclear Zeeman and hyperfine energies. **d**, An electron spin echo-detected field sweep showing the ESR spectrum of the triplet state. Resonances at different fields correspond to different molecular orientations with respect to the applied field. **e**, ENDOR spectroscopy is applied in four field positions to extract the isotropic hyperfine interaction between the triplet electron spin and the two nuclear spins ^{1}H and ^{31}P, measured to be 6 MHz and 11 MHz respectively.

and the principal values of the ZFS tensor $D_{xx} = 56$, $D_{yy} = 164$, $D_{zz} = -221$ MHz. These parameters depend on the spatial distribution of the triplet wavefunction and characterize the strength and asymmetry of the electron dipolar coupling. To determine the triplet populations and lifetime of the triplet sublevels we studied the echo intensity as a function of time after the laser pulse (see Supplementary Information). The extracted triplet state populations vary considerably according to the molecular orientation with respect to the applied magnetic field; however, typical values are $p_- = 0.2$, $p_0 = 0.6$ and $p_+ = 0.2$ as the initial populations of T_-, T_0 and T_+, indicating hyperpolarization well above the thermal polarization.

The hyperfine coupling between the triplet electron spin and the ^{1}H and ^{31}P nuclear spins can be measured using the Davies electron–nuclear double resonance (ENDOR) method[18], applied to select different molecular orientations within the sample. The spectra, shown in Fig. 1e, show narrow peaks around 6 and 14 MHz corresponding to the nuclear Larmor frequencies of the ^{31}P and ^{1}H spins, and arising from nuclear transitions in the T_0 subspace, where the hyperfine coupling is negligible (see Fig. 1c). The narrow linewidth of these peaks compared to the pulse excitation bandwidth enables high-fidelity control on these transitions.

The other peaks in the ENDOR spectra arise from the (orientation-dependent) hyperfine coupling in the $T_\pm$ subspaces. Fitting yields the isotropic hyperfine coupling terms $A(^{1}\mathrm{H}) = 6.0$ MHz and $A(^{31}\mathrm{P}) = 11$ MHz, consistent with density functional theory (DFT) modelling (see Supplementary Information). This hyperfine coupling allows conditional electron/nuclear spin operations to be performed; however, the breadth of these peaks (arising from the randomly oriented solid) results in poor fidelity nuclear spin control in the $T_\pm$ subspaces. Nevertheless, we will show that it is possible to apply entangling operations to states within the T_0 subspace, where there is negligible coupling between the nuclear and electron spins.

NMR experiments in the absence of optical excitation reveal the ground-state J-coupling between ^{31}P and ^{1}H to be 30 Hz, which leads to a nuclear controlled-NOT (CNOT) operation time of 17 ms. In the solid state, the dipolar coupling can be measured using the spin echo double resonance (SEDOR) pulse sequence[26,27], shown in Fig. 2a. SEDOR can be interpreted as a standard NMR CNOT operation modified to allow for initialization and readout by the electron spin. The timing of the refocussing pulses is swept to identify the optimum CNOT time of 160 μs,

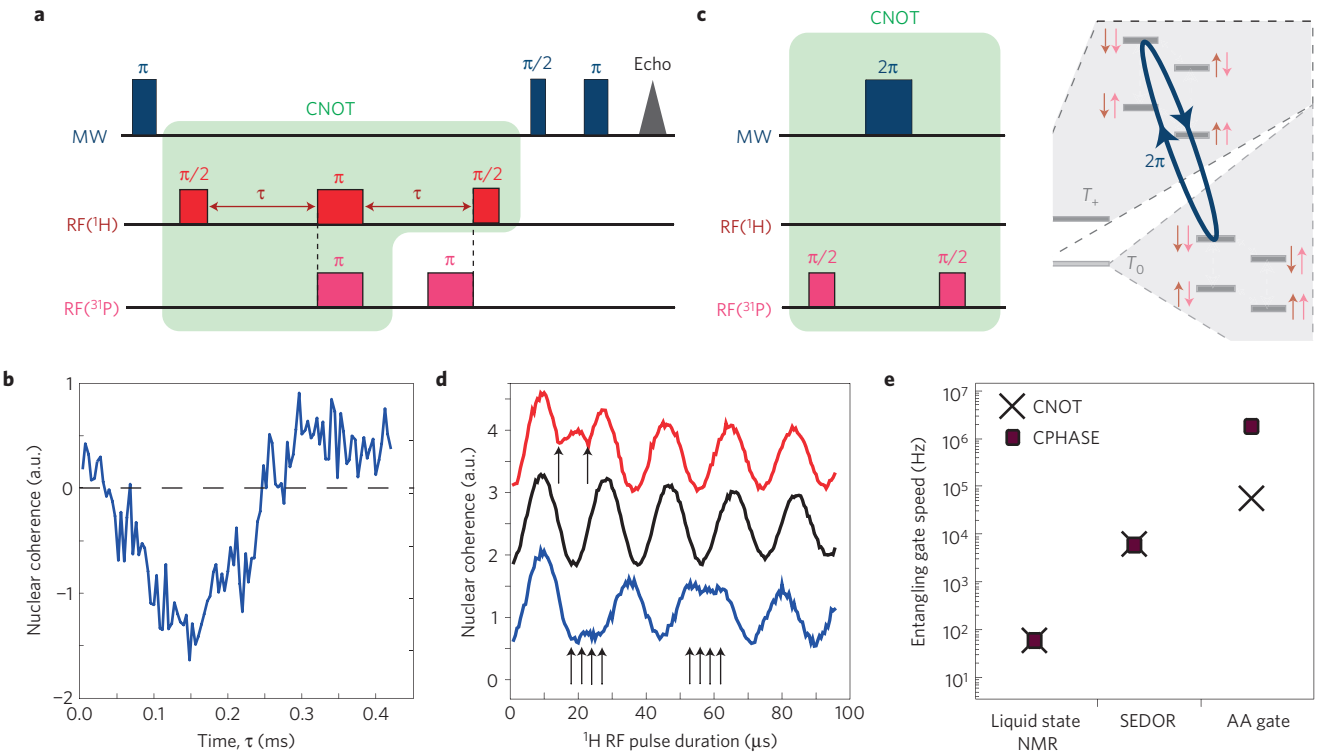

Figure 2 | Two different ways to implement nuclear spin entangling gates using the triplet electron spin. a, A technique based on the SEDOR sequence can be used to measure the dipolar coupling between spins. The sequence resembles a Hahn-echo experiment on one spin (^{1}H), however both spins are flipped during the refocussing pulse such that the sign of their coupling remains unchanged. Microwave pulses before and after are used to prepare and measure the ^{1}H nuclear spin coherence. **b**, The SEDOR sequence produces an oscillation in the nuclear coherence as τ is swept, corresponding to a nuclear coupling of 3 kHz. **c**, An alternative implementation of a CNOT gate consists of two Hadamard gates ($\pi/2$ pulses) and a CPHASE gate created by applying a selective 2π pulse to the electron spin. **d**, An ultrafast nuclear phase gate (created by a 2π microwave pulse) is applied during nuclear spin Rabi oscillations on the ^{1}H spin at points marked with arrows. Uninterrupted nuclear Rabi oscillations are shown in black. **e**, Comparison of the speed of the entangling operations. From the liquid state to the photoexcited solid state with the application of CPHASE gates there is an improvement of the entangling speed of five orders of magnitude.

corresponding to a 3 kHz nuclear coupling. By comparing this coupling time to the lifetime of the triplet state (approximately 0.5 ms) and nuclear T_2 times (0.20(4) and 1.9(4) ms for ^{1}H and ^{31}P respectively), we see that shorter entangling gate times are needed for higher fidelity operations. This can be achieved by using a triplet electron spin transition to apply an Aharanov–Anandan (AA; refs 7,28) controlled-phase (CPHASE) gate to the nuclear spins, as proposed in ref. 10.

If a quantum state is taken through a closed-loop trajectory in Hilbert space, it acquires a geometric phase equal to half the solid angle mapped out by that trajectory. A simple manifestation of this is a 2π pulse applied to a spin, which results in a global phase of π, consistent with its spinor nature, however more complicated trajectories are possible for other types of phase gates (see Supplementary Information). Because the microwave field is on-resonance with an electronic transition corresponding to a particular configuration of the ^{1}H and ^{31}P nuclear spins, we can apply a Toffoli gate: a microwave pulse which only rotates the electron spin when the nuclear spins are, say, in the $|\uparrow\uparrow\rangle$ state. Applying a 2π pulse to the electron in this way imparts a π phase shift to the $|\uparrow\uparrow\rangle$ state, with respect to the others in the T_0 subspace, equivalent to a CPHASE operation. Both the CPHASE and CNOT operations are well-defined with respect to an eigenbasis where $|4\rangle$ is the nuclear spin eigenstate associated with the chosen electronic transition. The eigenstates $|2\rangle$ and $|3\rangle$ differ from $|4\rangle$ by a ^{1}H and ^{31}P spin flip, respectively, and $|1\rangle$ differs from $|4\rangle$ by a flip of both nuclear spins. The relationship between these states $|1\rangle\cdots|4\rangle$ and a particular nuclear spin configuration (for example $|\uparrow\uparrow\rangle$) varies according to the molecular orientation (see Supplementary Information).

The duration of the CPHASE operation is limited only by the hyperfine coupling strength, which determines the minimum bandwidth of a selective microwave pulse, such that a CPHASE gate on a timescale of hundreds of nanoseconds can be performed. To illustrate how this phase gate can be applied to the individual nuclear spins, we applied 2π microwave pulses while driving nuclear Rabi oscillations (Fig. 2d). We verified that this CPHASE behaviour was conditional by observing uninterrupted Rabi oscillations on the complementary nuclear subspace. A CNOT operation can be built by combining the CPHASE gate with Hadamard rotations (Fig. 2c).

To compare the performance of these two entangling CNOT operations, we attempt to put the two nuclear spins into a Bell state and then perform tomography of the effective spin density matrix, building on methods described elsewhere[6] (see Supplementary Information). In short, each element of the density matrix must be mapped in turn onto the observable electron spin transition, through a combination of microwave and radiofrequency (RF) pulses. Notably, a CNOT (or similar) operation is needed when reading the zero- or double-quantum coherences (that is density matrix elements such as $|\uparrow\downarrow\rangle\langle\downarrow\uparrow|$ or $|\uparrow\uparrow\rangle\langle\downarrow\downarrow|$, respectively), and these can be accomplished using either of the methods introduced above. To improve the fidelity of the tomography, each element of the density matrix is imprinted with a particular time-varying phase applied to the nuclear spins

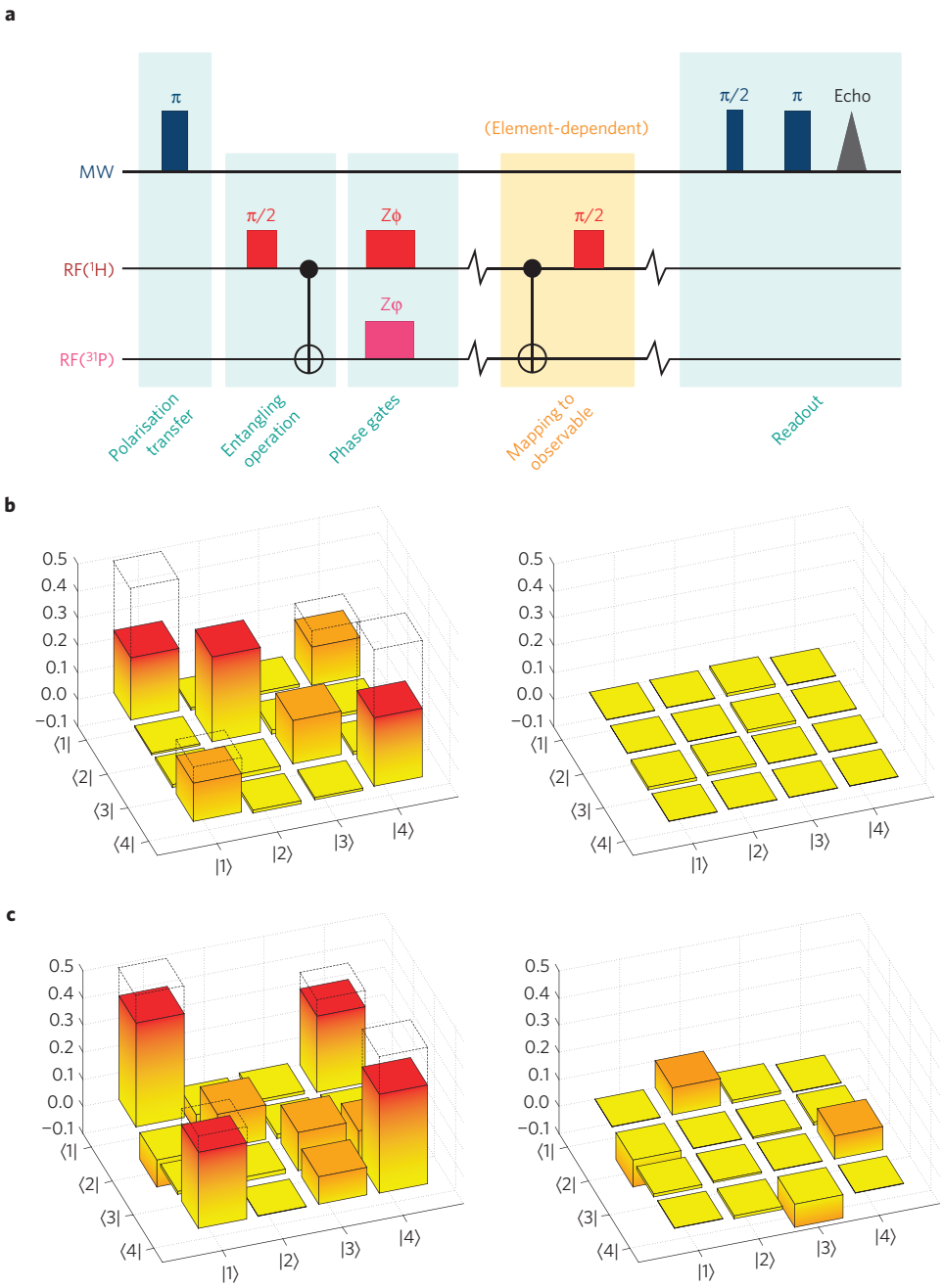

Figure 3 | Density matrix tomography results. a, General pulse sequence for the extraction of the $|1\rangle\langle 4|, |4\rangle\langle 1|$ elements of the density matrix, beginning with transfer of spin polarization from the triplet to the nuclear spins. The CNOT representations correspond to the entangling gates as represented by the shaded areas of Fig. 2a,b. The pulses mapping a density matrix element to the observable change depending on the density matrix element. **b**, Density matrix obtained using the entangling gates based on nuclear spin dipole coupling. The slow coupling leads to a fidelity of the operations of 34%. **c**, Density matrix obtained using CPHASE-based entangling gates. The ultrafast CPHASE gate entangles the nuclear spins in 220 ns and the fidelity increases to 65%. Uncertainties due to signal noise account for less than 0.005 and 0.002 on each density matrix element for the SEDOR- and CPHASE-based matrices, respectively (see Supplementary Information).

using RF pulses. The total pulse sequence for generating the pseudo-entangled state and measuring it using quantum state tomography is given in Fig. 3a.

In Fig. 3b,c we compare the density matrices obtained using the two different implementations of the CNOT gate: either exploiting the nuclear dipolar coupling in the solid state, or the triplet-mediated AA CPHASE operation combined with Hadamard gates. The fidelities of the final density matrices ρ_D with respect to the ideal Bell state ρ_B, calculated according to $F(\rho_B, \rho_D) = (\mathrm{Tr}(\sqrt{\sqrt{\rho_B}\rho_D\sqrt{\rho_B}}))^2$ are 34% and 65% respectively. The increased fidelity of the latter approach is due primarily to the much shorter gate times: the CPHASE entangling gate is performed in only 220 ns, and adding the Hadamard gates yields a CNOT gate time of 34.2 μs. In comparison, the CNOT based on the dipolar coupling had a duration of 160 μs. The maximum fidelities of each approach given the finite triplet recombination time for this molecule are 68% and 85%, respectively. The residual imperfection is due to the limited fidelity of the CPHASE operation (as evidenced in Fig. 2d by the loss of amplitude in the nuclear Rabi oscillations following the 2π microwave pulse) and small gate imperfections,

consistent with simulations incorporating a 4% error on each nuclear gate in the sequence.

The lifetime of the double quantum coherence is $T_{2,\mathrm{DQC}} \approx 100\,\mu s$ and the lifetime of the zero quantum coherence is $T_{2,\mathrm{ZQC}} \approx 200\,\mu s$, which indicates that they are limited by the hydrogen T_2 in the photoexcited state. Both nuclear coherence lifetimes in the liquid state are longer by orders of magnitude, which motivates the controlled removal of the electron spin in place of the stochastic decay process. Further improvements to the fidelity of the entangling gates and the polarization of the triplet state could be expected by using single-crystal samples allowing better orientation selection.

The approach demonstrated here can be readily applied to other systems where a transient electron spin can be coupled to multiple nuclear spins. Photoexcited triplet states offer the advantages of hyperpolarization, although methods for controlled de-excitation require further study. This could be achieved with the application of a second excitation to a higher order triplet state which undergoes reverse ISC to a singlet state[29]. Alternatively, charge separated states could be used to optically create a spin-1/2 electron on part of a molecule, and multiple excitations/chromophores could offer routes to controllably remove the spin. Finally, an electron spin may be controllably added and removed through electrostatic means in different systems, for example by ionizing/neutralizing a donor in silicon[30], which can couple to several ^{29}Si nuclear spins in addition to the donor nuclear spin.

Methods

Dimethyl[9-hydro(C_{60}-I_h)[5,6]fulleren-1(9H)-yl]phosphonate was prepared following the procedure reported in ref. 24, Scheme 1. Mono-functionalization of C_{60} was performed using dimethyl phosphonate in a solution of toluene and HMPA at 120 °C in the presence of oxygen. The product was purified by silica column chromatography (toluene, ramped to 10% ethyl acetate in toluene).

Pulsed electron spin resonance experiments were performed using an X-band (9–10 GHz) Bruker Elexsys680 spectrometer equipped with a low-temperature helium-flow cryostat (Oxford CF935). The arbitrary phase RF pulses were generated using a using a Rohde and Schwarz AFQ100B together with an Amplifier Research 500W amplifier. Photoexcitation was achieved using a Nd-YAG laser at 532 nm with 10 mJ pulses, 7 ns in length with a 10 Hz repetition rate.

Microwave pulse lengths were 128 ns for $\pi/2$ pulses, and 220 ns for both π and 2π pulses. The duration of RF pulses (both $\pi/2$ and π) was 17 µs. The samples were prepared in toluene-d8 with a concentration of 4×10^{-4} M, deoxygenated and flame-sealed under vacuum, and flash-frozen in liquid nitrogen.

Received 23 January 2012; accepted 25 May 2012; published online 1 July 2012

References

1. Cory, D. G., Fahmy, A. F. & Havel, T. F. Ensemble quantum computing by NMR spectroscopy. *Proc. Natl Acad. Sci. USA* **94,** 1634–1639 (1997).
2. Laflamme, R., Knill, E., Zurek, W. H., Catasti, P. & Mariappan, S. V. S. NMR Greenberger–Horne–Zeilinger states. *Phil. Trans. R. Soc. A* **356,** 1941–1948 (1998).
3. Morton, J. J. L. *et al.* Solid-state quantum memory using the ^{31}P nuclear spin. *Nature* **455,** 1085–1088 (2008).
4. Maly, T. *et al.* Dynamic nuclear polarization at high magnetic fields. *J. Chem. Phys.* **128,** 052211 (2008).
5. Barnes, A. B. *et al.* High-field dynamic nuclear polarization for solid and solution biological NMR. *Appl. Magn. Res.* **34,** 237–263 (2008).
6. Simmons, S. *et al.* Entanglement in a solid-state spin ensemble. *Nature* **470,** 69–72 (2011).
7. Morton, J. J. L. *et al.* Bang-bang control of fullerene qubits using ultrafast phase gates. *Nature Phys.* **2,** 40–43 (2006).
8. Hodges, J. S., Yang, J. C., Ramanathan, C. & Cory, D. G. Universal control of nuclear spins via anisotropic hyperfine interactions. *Phys. Rev. A* **78,** 010303 (2008).
9. Schaffry, M., Lovett, B. W. & Gauger, E. M. Creating nuclear spin entanglement using an optical degree of freedom. *Phys. Rev. A* **84,** 081305 (2011).
10. Robledo, L. *et al.* High-fidelity projective read-out of a solid-state spin quantum register. *Nature* **477,** 574–578 (2011).
11. Morton, J. J. L. & Lovett, B. W. Hybrid solid-state qubits: The powerful role of electron spins. *Annu. Rev. Condens. Matter Phys.* **2,** 1–54 (2011).
12. Kubo, Y. *et al.* Hybrid quantum circuit with a superconducting qubit coupled to a spin ensemble. *Phys. Rev. Lett.* **107,** 220501 (2011).
13. Barrett, S. D. & Kok, P. Efficient high-fidelity quantum computation using matter qubits and linear optics. *Phys. Rev. A* **71,** 060310 (2005).
14. Ryan, C. A., Emerson, J., Poulin, D., Negrevergne, C. & Laflamme, R. Characterization of complex quantum dynamics with a scalable NMR information processor. *Phys. Rev. Lett.* **95,** 250502 (2005).
15. Vandersypen, L. M. K. *et al.* Experimental realization of Shor's quantum factoring algorithm using nuclear magnetic resonance. *Nature* **414,** 883–887 (2001).
16. Jones, J. A. Quantum computing with NMR. *Prog. Nucl. Magn. Reson. Spectrosc.* **38,** 325–360 (2001).
17. Ryan, C. A., Moussa, O., Baugh, J. & Laflamme, R. Spin based heat engine: Demonstration of multiple rounds of algorithmic cooling. *Phys. Rev. Lett.* **100,** 140501 (2008).
18. Davies, E. R. A new pulse ENDOR technique. *Phys. Lett. A* **47,** 1–2 (1974).
19. Tyryshkin, A. M. *et al.* Coherence of spin qubits in silicon. *J. Phys.* **18,** S783–S794 (2006).
20. Khaneja, N. *et al.* Shortest paths for efficient control of indirectly coupled qubits. *Phys. Rev. A* **75,** 012322 (2007).
21. Mitrikas, G., Sanakis, Y. & Papavassiliou, G. Ultrafast control of nuclear spins using only microwave pulses: Towards switchable solid-state quantum gates. *Phys. Rev. A* **81,** 020305 (2010).
22. Zhang, Y., Ryan, C., Laflamme, R. & Baugh, J. Coherent control of two nuclear spins using the anisotropic hyperfine interaction. *Phys. Rev. Lett.* **107,** 170503 (2011).
23. Gauger, E. M., Rohde, P. P., Stoneham, A. M. & Lovett, B. W. Strategies for entangling remote spins with unequal coupling to an optically active mediator. *New J. Phys.* **10,** 073027 (2008).
24. Isobe, H., Chen, A-J., Solin, N. & Nakamura, E. Synthesis of hydrophosphorylated fullerene under neutral conditions. *Org. Lett.* **7,** 5633–5635 (2005).
25. Stoll, S. & Schweiger, A. EasySpin, a comprehensive software package for spectral simulation and analysis in EPR. *J. Magn. Reson.* **178,** 42–55 (2006).
26. Emshwiller, M., Hahn, E. & Kaplan, D. Pulsed nuclear resonance spectroscopy. *Phys. Rev.* **118,** 414–424 (1960).
27. Schweiger, A. & Jeschke, G. *Principles of Pulse Electron Paramagnetic Resonance* (Oxford Univ. Press, 2001).
28. Aharonov, Y. & Anandan, J. Phase change during a cyclic quantum evolution. *Phys. Rev. Lett.* **58,** 1593–1596 (1987).
29. Kamata, Y., Akiyama, K., Tero-Kubota, S. & Tabata, M. Two-laser two-color time-resolved EPR study on higher, excited-state triplet-singlet intersystem crossing of porphyrins and phthalocyanines. *Appl. Magn. Res.* **23,** 409–420 (2003).
30. Morello, A. *et al.* Single-shot readout of an electron spin in silicon. *Nature* **467,** 687–691 (2010).

Acknowledgements

We thank B. Lovett, M. Schaffry, E. Gauger, C. Kay, A. Ardavan, A. Briggs and D. Ceresoli for helpful discussions. This work was supported by the Engineering and Physical Sciences Research Council (EPSRC) through the Centre for Advanced Electron Spin Resonance (CAESR) (EP/D048559/1) and the Materials World Network (EP/I035536/1), as well as by the European Research Council (ERC) under the European Community's Seventh Framework Programme (FP7/2,007-2,013)/ERC grant agreement no. 279,781. We thank the Violette and Samuel Glasstone Fund, Clarendon Fund, John Templeton Foundation, St John's College, Oxford, and the Royal Society for support.

Author contributions

V.F., S.S. and J.J.L.M. designed and performed the experiments, analysed the results and wrote the manuscript. V.F. and F.G. performed the density functional calculations. S.D.K. and H.L.A. designed and synthesised the molecule. All authors discussed the results and manuscript.

Additional information

The authors declare no competing financial interests. Supplementary information accompanies this paper on www.nature.com/naturephysics. Reprints and permissions information is available online at www.nature.com/reprints. Correspondence and requests for materials should be addressed to J.J.L.M.